



Evaluating the effect of magnetocaloric properties on magnetic refrigeration performance

Engelbrecht, Kurt; Bahl, Christian Robert Haffenden

Published in:
Journal of Applied Physics

Link to article, DOI:
[10.1063/1.3525647](https://doi.org/10.1063/1.3525647)

Publication date:
2010

Document Version
Publisher's PDF, also known as Version of record

[Link back to DTU Orbit](#)

Citation (APA):
Engelbrecht, K., & Bahl, C. R. H. (2010). Evaluating the effect of magnetocaloric properties on magnetic refrigeration performance. *Journal of Applied Physics*, 108(12), 123918. <https://doi.org/10.1063/1.3525647>

General rights

Copyright and moral rights for the publications made accessible in the public portal are retained by the authors and/or other copyright owners and it is a condition of accessing publications that users recognise and abide by the legal requirements associated with these rights.

- Users may download and print one copy of any publication from the public portal for the purpose of private study or research.
- You may not further distribute the material or use it for any profit-making activity or commercial gain
- You may freely distribute the URL identifying the publication in the public portal

If you believe that this document breaches copyright please contact us providing details, and we will remove access to the work immediately and investigate your claim.

Evaluating the effect of magnetocaloric properties on magnetic refrigeration performance

K. Engelbrecht^{a)} and C. R. H. Bahl

Risø National Laboratory for Sustainable Energy, Frederiksborgvej 399, DK-4000 Roskilde, Denmark

(Received 19 August 2010; accepted 10 November 2010; published online 30 December 2010)

Active magnetic regenerator (AMR) refrigerators represent an alternative to vapor compression technology that relies on the magnetocaloric effect in a solid refrigerant. Magnetocaloric materials are in development and properties are reported regularly. Recently, there has been an emphasis on developing materials with a high entropy change with magnetization while placing lower emphasis on the adiabatic temperature change. This work uses model magnetocaloric materials and a numerical AMR model to predict how the temperature change and entropy change with magnetization interact and how they affect the performance of a practical system. The distribution of the magnetocaloric effect as a function of temperature was also studied. It was found that the adiabatic temperature change in a magnetocaloric material can be more important than the isothermal entropy change for certain conditions. A material that exhibits a sharp peak in isothermal entropy change was shown to produce a significantly lower cooling power than a material with a wide peak in a practical AMR system. © 2010 American Institute of Physics. [doi:10.1063/1.3525647]

I. INTRODUCTION

Active magnetic regenerative (AMR) refrigerators are a potentially environmentally friendly alternative to vapor compression technology that may be used for air-conditioning, refrigeration, and heat pump applications. Rather than using a gaseous refrigerant, AMRs use magnetocaloric materials (MCMs) that have a coupling between their thermodynamic properties and internal magnetic field. Assuming the material properties are independent of pressure the entropy of a MCM can be expressed as

$$ds = \frac{c_B}{T} dT + \left(\frac{\partial s}{\partial B} \right)_T dB, \quad (1)$$

where B is the magnetic field and c_B is the specific heat at constant magnetic field. As the magnetic field is increased the entropy of a MCM decreases as it moves to a more ordered state. Equation (1) illustrates that for a material with a positive magnetocaloric effect, the temperature of the material must increase when the material is magnetized adiabatically to maintain constant entropy. The magnitude of the temperature increase is related to the specific heat and the entropy change with magnetization of the material.

AMRs are a developing technology and there is much research effort currently focused on improving AMR performance. The properties of many new MCMs have been reported recently;¹ however, it is not certain which properties are most important when evaluating new materials. Several figures of merit for evaluating magnetocaloric properties have been proposed, but these figures ignore important aspects of the AMR cycle. This paper investigates several important magnetocaloric properties and demonstrates their effect on AMR performance.

The earliest magnetic refrigerators used a one-shot demagnetization cycle with a temperature span that was limited by the adiabatic temperature change of the MCM. Such a device was used to create a cooling device able to cool below 1 K.² The operating temperature span of magnetic refrigerators can be dramatically increased by using a regenerative cycle, as demonstrated by Ref. 3. Since 1976, many new devices have been reported,⁴ with modern AMRs generally using permanent magnets with regenerators made of packed spheres, packed particles, or parallel plates of MCM. The AMR cycle uses a heat transfer fluid to transport the heat generated from magnetizing and demagnetizing the MCM to the hot and cold reservoirs. The AMR cycle has four basic processes: magnetization, the cold-to-hot blow, demagnetization, and the hot-to-cold blow. During magnetization, the temperature of the MCM increases, then fluid is pumped from the cold reservoir to the hot reservoir in order to reject the magnetic work to ambient. The regenerator is then demagnetized, causing a decrease in temperature and a cooling load is accepted from the cooled space by pumping fluid from the hot reservoir across the regenerator and into the cold reservoir. The system performance is mostly a function of the MCM, heat transfer characteristics in the regenerator, and cycle parameters such as frequency and fluid flow rate.

Developing and characterizing new MCMs is an active research topic and the properties of many new compositions are reported each year.⁵ The two most cited properties for potential AMR materials are the adiabatic temperature change with magnetization, ΔT_{ad} , and the isothermal entropy change with magnetization, Δs_{mag} . Much of the recent research has focused on developing first order magnetic transition (FOMT) materials that exhibit high Δs_{mag} but often have lower ΔT_{ad} than second order transition materials such as Gd. Some FOMT materials of interest that have recently been reported are Gd₅Si₂Ge₂,⁶ La(Fe, Si)₁₃,⁷ and MnFe(P and

^{a)}Electronic mail: kuen@risoe.dtu.dk.

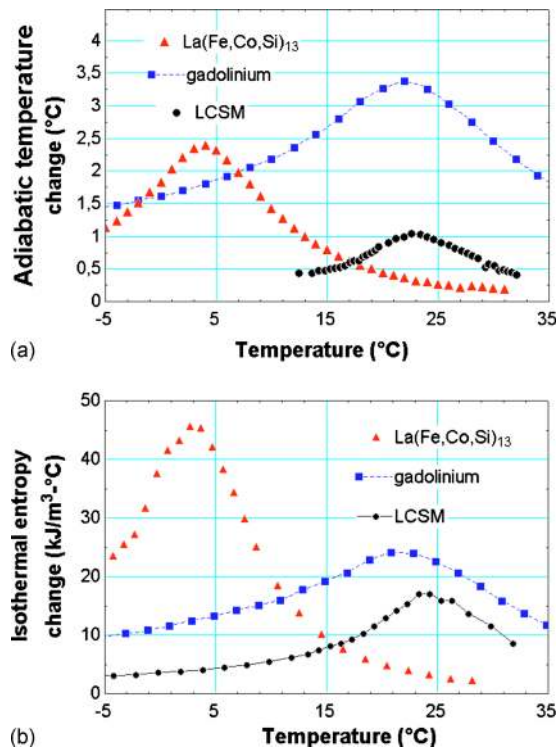


FIG. 1. (Color online) The adiabatic temperature change (a) and volumetric isothermal entropy change (b) of $\text{LaFe}_{11.06}\text{Co}_{0.86}\text{Si}_{1.08}$ gadolinium (Gd), and $\text{La}_{0.67}\text{Ca}_{0.26}\text{Sr}_{0.07}\text{Mn}_{1.05}\text{O}_3$ (an LCSM compound) when magnetized from 0 to 1 T as a function of temperature (Ref. 13).

As).⁸ Many recent publications on MCM properties (such as Ref. 9) report only Δs_{mag} without ΔT_{ad} or the specific heat while others present both properties (Refs. 10–12 among others). However, it is not well understood how the combination of the two properties affect practical AMR performance or what ideal MCM properties are. This paper uses a one-dimensional (1D) numerical model of a simple AMR system to predict how variations in ΔT_{ad} and Δs_{mag} interact and which MCM properties are more desirable for AMR applications.

The magnetocaloric effect for most materials exhibiting a large effect near room temperature is highly temperature dependent. Δs_{mag} and ΔT_{ad} as a function of temperature as reported by Ref. 13 for three candidate MCMs are shown in Fig. 1. The figure shows that magnetocaloric properties are generally highly nonlinear and that the magnitude of Δs_{mag} and ΔT_{ad} can differ significantly between materials, due to differences in the value of the specific heat for each material. The figure shows that Gd has a relatively high ΔT_{ad} but a moderate Δs_{mag} . Gd is the most common MCM reported in AMR prototypes to date⁴ and the highest operating temperature spans are generally achieved using regenerators made of Gd and its alloys, such as $\text{Gd}_{1-x}\text{Er}_x$ or $\text{Gd}_{1-x}\text{Tb}_x$.¹⁴

A. Thermal processes in an AMR

The thermal and hydraulic interactions in an AMR device are the same as those described for passive regenerator applications¹⁵ with the addition of a magnetic interaction term. Including magnetic interaction terms and considering the equations only in the fluid flow direction, the 1D AMR

governing equations are shown below. The governing equations for the fluid phase in an AMR are given in Eq. (2) with subscripts f and s indicating fluid and solid.

$$\dot{m}_f c_f \frac{\partial T_f}{\partial x} + h A_{\text{HT}} (T_f - T_s) + \rho_f A_c \epsilon c_f \frac{\partial T_f}{\partial t} - k_{\text{disp}} A_c \frac{\partial^2 T_f}{\partial x^2} = 0, \quad (2)$$

where T is temperature, ρ is density, c is specific heat, h is the heat transfer coefficient, A_{HT} is the area for heat transfer, ϵ is the porosity, \dot{m}_f is the fluid mass flow rate, and A_c is the cross sectional area. The terms represent (in order from left to right) the enthalpy change in the flow, heat transfer from the fluid to the solid, energy storage, and energy transfer due to axial dispersion associated with mixing of the fluid. Viscous dissipation due to pumping losses is ignored. The governing equation for the solid regenerator material is

$$h A_{\text{HT}} (T_f - T_s) + k_{\text{eff}} \frac{\partial^2 T_s}{\partial x^2} = (1 - \epsilon) \rho_s T_s \left(\frac{\partial s_s}{\partial B} \right)_T \frac{\partial B}{\partial t} + (1 - \epsilon) \rho_s c_{B,s} \frac{\partial T_s}{\partial t}, \quad (3)$$

where B is the internal magnetic field of the solid regenerator and k_{eff} is the effective thermal conductivity of the fluid and solid matrix. The terms represent heat transfer from the fluid to the regenerator, nondispersive, or static axial conduction (through the composite of the regenerator and fluid), magnetic work transfer, and energy storage.

Examination of Eqs. (2) and (3) reveals that the most important physical interactions in an AMR device are the magnetocaloric effect in the solid material, heat transfer between the fluid and solid, energy storage in the solid and fluid phases, and axial conduction through the regenerator from the hot reservoir to the cold reservoir. Pumping losses are ignored in this study because they are dependent on regenerator geometry and operating conditions and not directly to magnetocaloric properties. The effect of varying axial conduction losses is not considered to reduce the parameter space. This work considers how MCM selection affects AMR performance through heat transfer from the solid to the fluid and the magnetic work into the system. The magnetic work term is straightforward, as it is directly proportional to Δs_{mag} of the material and the magnetic field change, but ΔT_{ad} also plays an important role in increasing the temperature difference between the solid and fluid and facilitates heat transfer between the fluid and solid across a temperature span and heat rejection to a warmer thermal reservoir. Thermal storage in the solid is also important because the specific heat of MCMs can vary widely.¹

B. Current methods to evaluate MCMs

As new MCMs are fabricated and characterized, it is necessary to compare them to the current state of the art materials. There are several methods currently used to estimate the potential performance of a MCM used in a magnetic refrigerator. The first is to simply integrate the isothermal entropy change with magnetization over the working

temperature span of the regenerator¹ [Eq. (4)]. This is referred to as the refrigeration capacity of the material

$$R_{\text{CAP}} = \int_{T_C}^{T_H} \Delta s_{\text{mag}}(T) dT. \quad (4)$$

Another method is to calculate the relative cooling power, RCP , of the material.¹⁶ RCP is defined as the product of the peak value of Δs_{mag} and the temperature range at half maximum, ΔT_{THM} , which is defined as the temperature span between the two points where the entropy change with magnetization is half the peak value

$$RCP = \Delta s_{\text{mag,MAX}} \Delta T_{\text{THM}}. \quad (5)$$

In the regenerative cycle, there is a temperature gradient from the cold reservoir to the hot reservoir in the direction of flow after steady state has been achieved. The temperature gradient in the solid material means that each location along the flow direction of the regenerator is potentially at a different temperature, and, therefore, undergoes a unique thermodynamic cycle. Neither of the techniques described above accounts for the different cycle experienced by each position in the regenerator and at times do not adequately describe the magnetocaloric properties of a material used in an AMR. The figures of merit from Eqs. (4) and (5) ignore the heat transfer process between the solid and fluid in an AMR and can, therefore, be misleading when evaluating an MCM. The refrigeration capacity, R_{CAP} is positive for any given temperature span, even if ΔT_{ad} is zero for a large portion of the operating temperature. The RCP of a material is independent of operating temperatures and is only applicable when the material operates near its Curie temperature. The remainder of this work studies how both ΔT_{ad} and Δs_{mag} affect the performance of a practical AMR.

II. MCM PROPERTIES

Because the purpose of this work is to study the effects of varying properties on AMR performance, it is most convenient to use modeled materials. Examining Eqs. (2) and (3), the solid material properties that are relevant for an AMR are density, thermal conductivity, specific heat at constant magnetic field, ΔT_{ad} , and Δs_{mag} . The density and thermal conductivity are both held constant for all materials in this work. The specific heat, ΔT_{ad} and Δs_{mag} are coupled through the entropy curves, and if two are specified, the third can be calculated. Assuming the MCM properties are independent of pressure, the zero-field entropy of the material can be calculated by integrating the assumed zero-field specific heat

$$s(T, B=0) = \int_0^T \left(\frac{c_{\text{B},s}}{T} dT \right). \quad (6)$$

The entropy for each magnetic field is then calculated by either shifting the zero-field entropy along the temperature axis by ΔT_{ad} or shifting it along the entropy axis by Δs_{mag} . The specific heat at nonzero magnetic fields must be calculated from the entropy curve at the desired field. Three sets of MCMs were studied: a set with constant R_{CAP} , constant Δs_{mag} and varying ΔT_{ad} , a set with constant ΔT_{ad} and varying

TABLE I. Magnetocaloric characteristics of a series of materials with constant adiabatic temperature change and varying specific heat.

Material	Specific heat (J/kg K)	ΔT_{ad} (K)	Δs_{mag} (avg) (J/kg K)	R_{CAP} (J/kg)
1	250	4	-3.5	51.6
2	500	4	-7.0	103.3
3	1000	4	-14.0	206.6
4	1500	4	-21.1	309.9

Δs_{mag} and thus varying R_{CAP} , and a set with Lorentzian distributions of Δs_{mag} and constant ΔT_{ad} and constant R_{CAP} . The sets of modeled properties can be used to study the effect on AMR performance of varying ΔT_{ad} , Δs_{mag} , and the shape of the Δs_{mag} curve, respectively, while the other pertinent material properties are held constant. The properties of the materials with intermediate values were chosen to be similar to Gd or a composition of $\text{La}(\text{Fe}, \text{Co}, \text{Si})_{13}$ but the extreme properties are strictly theoretical. For example, no material with a ΔT_{ad} of 13.8 K at 2 T is currently known, but it is of interest to model.

The magnetocaloric properties of the first two sets of materials that are used for AMR system simulations are summarized in Tables I and II. R_{CAP} was calculated for each material assuming the AMR operates between 285 and 300 K. The values of ΔT_{ad} and Δs_{mag} were chosen to be on the same order of magnitude as Gd (Ref. 17) or $\text{La}(\text{Fe}, \text{Si})_{13}$ (Ref. 18) for a maximum magnetic field of 2 T. The thermal conductivity for each material was set to a temperature-independent value of 10 W/m K based on property measurements by.¹⁹

Tables I and II illustrate the relationship between specific heat, ΔT_{ad} , and Δs_{mag} . For a given Δs_{mag} , ΔT_{ad} decreases as the specific heat increases while R_{CAP} remains constant.

The final material set was developed to study how the shape of the magnetocaloric effect as a function of temperature affects AMR performance. For this study, the shape of the Δs_{mag} curve illustrated in Fig. 1 is approximated as a Lorentzian curve with an assumed Curie temperature. To fully specify the magnetocaloric properties, ΔT_{ad} is assumed to be a constant value of 4 K and R_{CAP} is set to 103 J/kg, corresponding to material 2 from Table I. The formula used to calculate the zero-field heat capacity is given in Eq. (7)

$$c_{\text{B}=0,s} = \frac{c_{\text{peak}}}{\pi} \frac{\Gamma}{(T - T_{\text{Curie}})^2 + \Gamma^2}, \quad (7)$$

where Γ is a parameter that determines the width of the specific heat curve. Because ΔT_{ad} is assumed constant for

TABLE II. Magnetocaloric characteristics of a series of materials with constant entropy change with magnetization and varying specific heat.

Material	Specific heat (J/kg K)	ΔT_{ad} (avg) (K)	Δs_{mag} (J/kg K)	R_{CAP} (J/kg)
1	125	13.8	-6	90
2	250	6.8	-6	90
3	500	3.4	-6	90
4	1000	1.7	-6	90

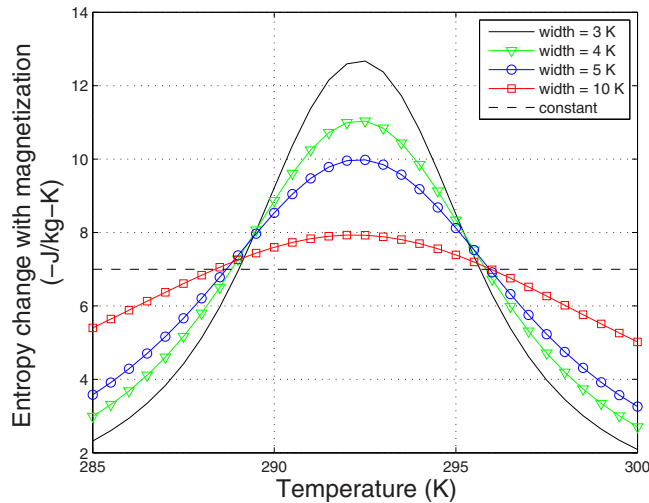


FIG. 2. (Color online) The entropy change with magnetization as a function of temperature for several materials listed in Table III.

these materials, the zero-field specific heat calculated in Eq. (7) determines the Δs_{mag} curve. The term c_{peak} is determined iteratively for each value of Γ by varying the value until the desired value of R_{CAP} is achieved.

Material properties were modeled for Γ values of 3, 4, 5, and 10. Material 2 from Table I can be considered part of the final set with a Γ that approaches infinity. The Curie temperature, as defined by the temperature where Δs_{mag} is maximum, of all materials in the final set is set to 292.5 K, which is the average of the hot and cold reservoir temperatures. A plot of the calculated Δs_{mag} curves for the materials from this final material set is shown in Fig. 2 and a summary of the materials is given in Table III.

III. NUMERICAL MODELING TECHNIQUE

The nonlinear nature of magnetocaloric properties makes numerical modeling of an AMR system necessary. Several detailed AMR models have been presented recently, including 1D porous models (e.g., Refs. 20–23), two-dimensional (2D) models of parallel plate regenerators,^{24,25} a 2D porous model,²⁶ and a full three-dimensional (3D) model.²⁷ Porous models require correlations to calculate heat transfer and pressure drop inside the regenerator bed, while the 2D plate models and the 3D model solve the coupled fluid flow and heat transfer equations directly. Beside the geometry modeled, the different models often use different approaches to implement the magnetocaloric effect in the solid material. Many models treat the magnetocaloric effect as a heat source

TABLE III. Magnetocaloric characteristics of a series of materials with constant refrigeration capacity and varying standard deviation of entropy change with magnetization.

Material	Std. dev. (K)	ΔT_{ad} (K)	Max. Δs_{mag} (J/kg K)	R_{CAP} (J/kg)
1	3	4	-10.0	103
2	4	4	-10.1	103
3	5	4	-9.4	103
4	10	4	-7.4	103

term that varies with change in the magnetic field (e.g., Refs. 23 and 24) while others treat it as an instantaneous change in the solid temperature (e.g., Refs. 20 and 21). Because the AMR system that is modeled is not specific, the model used is not highly important. The 1D numerical model by Ref. 23 was chosen because it allows the regenerator material properties to be specified relatively easily and the computational requirements are not prohibitive. The model was verified experimentally against results for the AMR device described by Ref. 28 and good agreement between predicted and experimental results were achieved.²³

The model used in this paper assumes that the fluid and solid temperature profiles are functions of only the x -direction (flow direction) and that there is a uniform fluid flow in the flow channels. The regenerator housing and ends ($x=0$, and $x=L$) are assumed adiabatic. During the blow periods the fluid enters the regenerator with the prescribed temperature of the hot thermal reservoir (T_H) or the cold reservoir (T_C), and the system operates at steady state. AMR performance is determined by solving the coupled 1D partial differential equations in space and time describing the temperature in the regenerator and in the fluid. Established correlations are used to determine important regenerator parameters such as the heat transfer between solid and fluid phases and thermal axial conduction. The model is flexible with respect to operating conditions, geometry, and material and fluid properties. The equipment external to the regenerator bed (e.g., the pumps, drive motor, etc.) are not explicitly modeled; their effect on the bed is felt through an imposed time variation in the fluid mass flow rate and magnetic field. The magnetic field profile is the same for each simulation while the fluid flow rate is varied. The numerical model starts from an initial temperature distribution and takes implicit time steps forward in time until cyclical steady state has been achieved. Steady state is defined as when the dimensionless value of the absolute change in energy of the regenerator from cycle to cycle is less than a specified tolerance. The 1D model has been implemented in MATLAB and the code may be downloaded at the following web address: <http://sel.me.wisc.edu/publications.shtml>.

The regenerator geometry modeled in this work is a packed sphere regenerator with either 0.25 mm diameter spheres or 0.50 mm diameter spheres. The heat transfer between the regenerator and fluid is determined from the Nusselt number, which is determined from the correlation suggested by Ref. 29 for heat transfer in a packed sphere bed. The modeled regenerator has a length of 60 mm and a cross sectional area of 4 cm². The heat transfer fluid is water with constant properties. The cycle parameters used as inputs to the AMR model are shown in Table IV. The dwell ratio is the fraction of the cycle when there is no fluid flow for a given regenerator bed.

IV. RESULTS AND DISCUSSION

The model was run for regenerators with 0.25 and 0.50 mm sphere diameters (corresponding to approximately 0.1 and 0.2 mm hydraulic diameters) for a range of fluid flow rates for the set of materials listed in Table I. The predicted

TABLE IV. Process parameters inputs for the numerical AMR model.

Parameter	Value	Unit
Cold reservoir temp (T_C)	285	K
Hot reservoir temp (T_H)	300	K
Cycle period (τ)	0.5	s
Dwell ratio	1/3	
Sphere diameter	0.25, 0.5	mm
Porosity (ϵ)	0.36	
Magnetic field	2	T
Regenerator volume	24	cm ³
MCM mass	121	g
Fluid flow rate (\dot{m}_f)	varied	

cooling power as a function of fluid flow rate is shown in Fig. 3. The fluid flow rates in this section are normalized by the volume of fluid to the total regenerator volume. They are intentionally not presented as a function of regenerator utilization to illustrate how the fluid flow rate varies with each material

$$\bar{V} = \frac{\dot{m}_f \rho_f}{A_c L}, \tag{8}$$

where L is the length of the regenerator. The normalized flow rate indicates how many times the volume of the regenerator could be replaced by the fluid per second.

The results in Fig. 3 show some interesting trends. If ΔT_{ad} is held constant and the specific heat is increased (raising Δs_{mag}), the cooling capacity of the system increases for

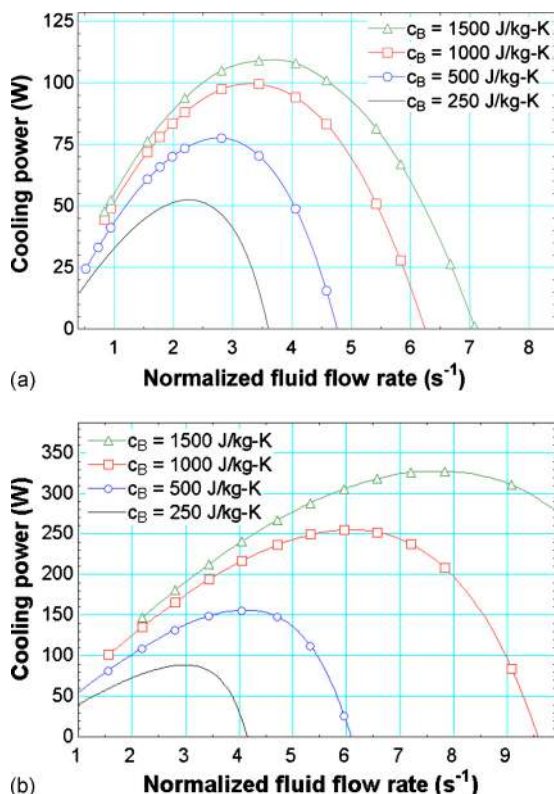


FIG. 3. (Color online) The refrigeration capacity as a function of normalized flow rate for materials with a constant ΔT_{ad} and varying specific heat for an AMR with (a) 0.5 mm and (b) 0.25 mm spheres.

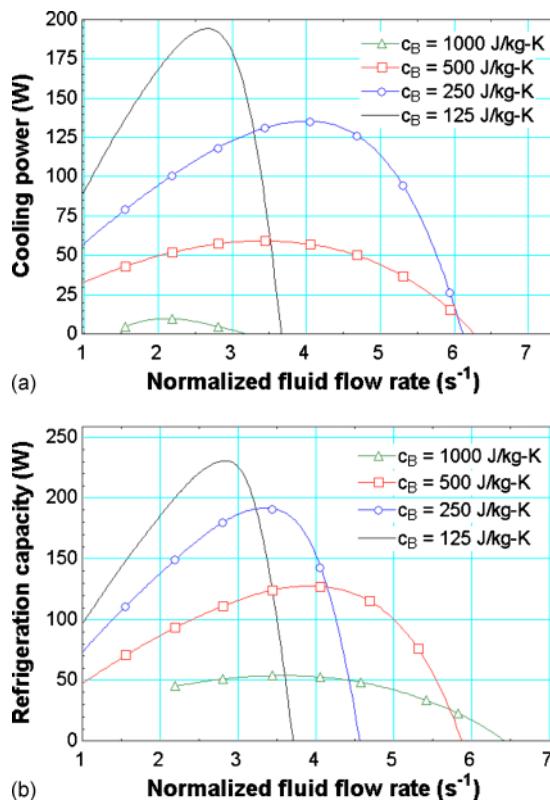


FIG. 4. (Color online) The refrigeration capacity as a function of normalized flow rate for materials with a constant Δs_{mag} and varying specific heat for an AMR with (a) 0.5 mm and (b) 0.25 mm spheres.

all flow rates, but the flow rate must increase significantly to realize the full potential of the materials with higher thermal mass. The effect of increasing Δs_{mag} while holding ΔT_{ad} constant is highly dependent on regenerator geometry. Figure 3 shows that the increase in cooling capacity with increasing specific heat is much greater for the regenerator with a smaller sphere size and higher heat transfer area. Because regenerators made from MCMs with high specific heat require high fluid flow rates, pumping losses will also increase and may become a significant loss mechanism.

The same procedure was performed on the set of material properties with constant Δs_{mag} and varying specific heat and, therefore, varying ΔT_{ad} and the results are shown in Fig. 4.

Figure 4 shows that AMR performance is significantly influenced by ΔT_{ad} of the material, even when R_{CAP} is held constant. As the specific heat increases, ΔT_{ad} and the refrigeration capacity tend toward zero. Materials with high ΔT_{ad} but low specific heat perform well at low fluid flow rates, but quickly become overwhelmed and are not suitable for high flow rate applications. Results for this set of materials also show that ΔT_{ad} is a more important property for regenerators with lower heat transfer performance, i.e., the regenerator with larger sphere diameter. AMR systems using materials with high ΔT_{ad} and low specific heat also have the advantage of being able to generate high cooling power at low fluid flow rates. This illustrates that heat transfer between the solid and fluid is an important phenomenon in AMR systems and

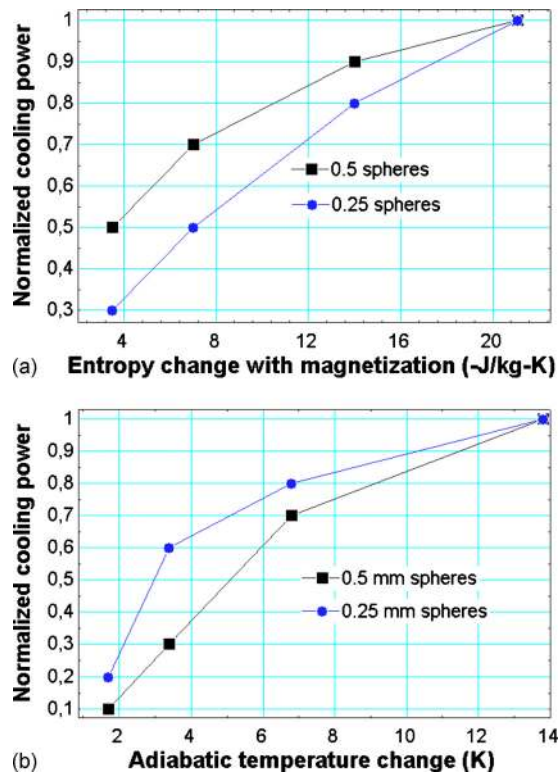


FIG. 5. (Color online) The normalized maximum refrigeration capacity as a function of (a) Δs_{mag} and (b) ΔT_{ad} for an AMR with 0.5 and 0.25 mm spheres.

cannot be ignored when evaluating MCM properties. Figures 3 and 4 are summarized in Fig. 5 by normalizing the cooling capacity for each set of material.

The cooling power in Fig. 5 was normalized so that the maximum cooling power produced for each series is equal to one to study the relative impact of changes in either ΔT_{ad} or Δs_{mag} on each system. The figure shows that the cooling power of regenerators with relatively low heat transfer performance is more dependent on ΔT_{ad} than Δs_{mag} , as a 50% reduction in ΔT_{ad} reduces cooling power by approximately 30% while a 67% reduction in Δs_{mag} is needed for the same reduction in cooling power. The regenerator with smaller spheres is more sensitive to Δs_{mag} , as it has the ability to transfer the magnetic work over a smaller temperature difference between the solid and fluid. However, both regenerators in Fig. 5 are highly dependent on ΔT_{ad} of the regenerator material. Experiments on prototype AMR system have suggested that Gd regenerators often outperform similar devices that use materials with higher Δs_{mag} but lower ΔT_{ad} .⁴

Finally, the AMR performance for materials with constant R_{CAP} and varying shapes of the magnetocaloric effect was predicted, and the results are shown in Fig. 6. The figure shows that the material with the highest performance is that with a constant Δs_{mag} . Cooling capacity can decrease by 50% for materials with the same R_{CAP} due to the shape of the specific heat and Δs_{mag} curves. One explanation for this phenomenon is that the magnetocaloric effect is unevenly distributed when the material shows a pronounced peak in Δs_{mag} with respect to temperature. Because the heat transfer and fluid flow are equal throughout the regenerator, portions

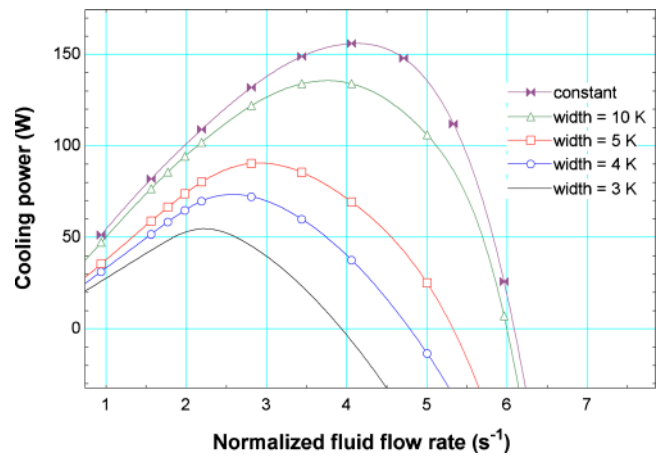


FIG. 6. (Color online) The cooling power as a function of normalized fluid flow rate for the material set listed in Table III for a regenerator with 0.25 mm spheres.

of the bed operating at temperatures further away from the Curie temperature underperform relative to other parts of the regenerator and the system performance decreases. Therefore, for a single material regenerator, MCMs with sharp peaks in the magnetocaloric effect are less attractive than those with an equal R_{CAP} and a more evenly distributed magnetocaloric effect.

The results presented here are for packed sphere regenerators but the general findings should also apply to parallel plate regenerators or other regenerator geometries. Studying the governing equations for the AMR system shows that the most important regenerator parameters are heat transfer performance and heat capacities of the solid and fluid. Therefore, any AMR system using similar materials and regenerators with similar heat transfer performance should exhibit the same trends. Pressure drop and axial conduction losses were not considered in this study, and those losses would not affect results presented in this paper if alternative regenerator geometries were modeled.

V. CONCLUSIONS

The effect of varying Δs_{mag} and ΔT_{ad} were investigated using a 1D numerical AMR model. The results showed that the cooling power even for regenerators with high heat transfer performance (a regenerator of packed 0.25 mm spheres) is highly dependent on ΔT_{ad} of the regenerator material. This indicates that reporting Δs_{mag} alone is not sufficient for characterizing MCMs and the common techniques to predict AMR performance based only on Δs_{mag} data such as R_{CAP} or RCP ignore the important heat transfer interaction between the solid and fluid in an AMR. The numerical simulations performed in this work also suggest that ΔT_{ad} is more important than Δs_{mag} when the fluid flow rate is relatively low or the heat transfer effectiveness in the regenerator is low. Because materials with high Δs_{mag} and high specific heat require larger fluid flow rates to realize their performance potential, pumping losses may become large and reduce system efficiency.

Finally, it was shown that materials with pronounced spikes in Δs_{mag} show reduced performance compared to ma-

terials with constant Δs_{mag} and equal R_{CAP} . This could make materials that exhibit a large peak in Δs_{mag} over a narrow temperature band less desirable for AMR applications, especially for a single material regenerator. MCM research should emphasize developing materials with high ΔT_{ad} over a broad temperature range rather than solely increasing peak values of Δs_{mag} .

ACKNOWLEDGMENTS

The authors would like to acknowledge the support of the Programme Commission on Energy and Environment (EnMi) (Contract No. 2104-06-0032) which is part of the Danish Council for Strategic Research.

- ¹K. A. Gschneidner, Jr., V. K. Pecharsky, and A. O. Tsokol, *Rep. Prog. Phys.* **68**, 1479 (2005).
- ²W. F. Giauque and D. P. MacDougall, *Phys. Rev.* **43**, 768 (1933).
- ³G. Brown, *J. Appl. Phys.* **47**, 3673 (1976).
- ⁴B. Yu, M. Liu, P. W. Egolf, and A. Kitanovski, *Int. J. Refrig.* **33**, 1029 (2010).
- ⁵K.A. Gschneidner, Jr. and V. Pecharsky, *Int. J. Refrig.* **31**, 945 (2008).
- ⁶K. A. Gschneidner, Jr. and V. K. Pecharsky, *Phys. Rev. Lett.* **85**, 4190 (2000).
- ⁷A. Fujita, S. Fujieda, Y. Hasegawa, and K. Fukamichi, *Phys. Rev. B* **67**, 104416 (2003).
- ⁸E. Brück, M. Ilyn, A. M. Tishin, and O. Tegus, *J. Magn. Magn. Mater.* **290–291**, 8 (2005).
- ⁹L. Mañosa, D. González-Alonso, A. Planes, E. Bonnot, M. Barrio, J.-L. Tamarit, S. Aksoy, and M. Acet, *Nature Mater.* **9**, 478 (2010).
- ¹⁰J. Lyubina, R. Schäfer, N. Martin, L. Schultz, and O. Gutfleisch, *Adv. Mater. (Weinheim, Ger.)* **22**, 3735 (2010).
- ¹¹B. R. Hansen, L. T. Kuhn, C. R. H. Bahl, M. Lundberg, C. Ancona-Torres, and M. Katter, *J. Magn. Magn. Mater.* **322**, 3447 (2010).
- ¹²S. A. Nikitin, K. P. Skokov, Y. S. Koshik'ko, Y. G. Pastushenkov, and T. I. Ivanova, *Phys. Rev. Lett.* **105**, 137205 (2010).
- ¹³R. Bjørk, C. Bahl, and M. Katter, *J. Magn. Magn. Mater.* **322**, 3882 (2010).
- ¹⁴A. Rowe and A. Tura, *Int. J. Refrig.* **29**, 1286 (2006).
- ¹⁵H. Hausen, *Heat Transfer in Counterflow, Parallel-Flow and Cross-Flow* (McGraw-Hill, New York, 1983).
- ¹⁶A. M. Tishin and Y. I. Spichkin, *The Magnetocaloric Effect and its Applications* (Institute of Physics, Temple Back, Bristol, UK, 2003).
- ¹⁷S. Dan'kov, A. Tishin, V. Pecharsky, and K. A. Gschneidner, Jr., *Phys. Rev. B* **57**, 3478 (1998).
- ¹⁸A. Fujita, Y. Akamatsu, and K. Fukamichi, *J. Appl. Phys.* **85**, 4756 (1999).
- ¹⁹S. Fujieda, Y. Hasegawa, A. Fujita, and K. Fukamichi, *J. Appl. Phys.* **95**, 2429 (2004).
- ²⁰M. Risser, C. Vasile, T. Engel, B. Keith, and C. Muller, *Int. J. Refrig.* **33**, 973 (2010).
- ²¹G. Tagliafico, F. Scarpa, and F. Canepa, *Int. J. Refrig.* **33**, 286 (2010).
- ²²S. Jacobs, in Proceedings of the Third International Conference Magnetic Refrigeration at Room Temperature, Des Moines, Iowa, USA, 2009, p. 267.
- ²³K. Engelbrecht, A numerical model of an active magnetic regenerator refrigerator with experimental validation, Ph.D. thesis, University of Wisconsin, 2008.
- ²⁴K. Nielsen, C. Bahl, A. Smith, N. Pryds, and J. Hattel, *Int. J. Refrig.* **33**, 753 (2010).
- ²⁵P. A. Oliveira, P. Trevizoli, J. R. Barbosa, Jr., and A. Prata, Proceedings of the Third International Conference on Magnetic Refrigeration at Room Temperature, Des Moines, Iowa, USA, 2009, p. 283.
- ²⁶M. Liu and B. F. Yu, in Proceedings of the Fourth International Conference on Magnetic Refrigeration at Room Temperature, Baotou, Inner Mongolia, China, 2010, p. 477.
- ²⁷J. Bouchard, H. Nesreddine, and N. Galanis, *Int. J. Refrig.* **52**, 1223 (2009).
- ²⁸C. Zimm, A. Boeder, J. Chell, A. Sternberg, A. Fujita, S. Fujieda, and K. Fukamichi, *Int. J. Refrig.* **29**, 1302 (2006).
- ²⁹M. Kaviany, *Principles of Heat Transfer in Porous Media* (Springer, New York, 1995).